HOKKAIDO UNIVERSITY

Title	A theoretical cell-killing model to evaluate oxygen enhancement ratios at DNA damage and cell survival endpoints in radiation therapy
Author(s)	Matsuya, Yusuke; Sato, Tatsuhiko; Nakamura, Rui et al.
Citation	Physics in medicine and biology, 65(9), 095006 https://doi.org/10.1088/1361-6560/ab7d14
Issue Date	2020-04-27
Doc URL	https://hdl.handle.net/2115/81071
Rights	This is an author-created, un-copyedited version of an article published in Physics in Medicine and Biology. IOP Publishing Ltd is not responsible for any errors or omissions in this version of the manuscript or any version derived from it. The Version of Record is available online at https://doi.org/10.1088/1361-6560/ab7d14.
Type	journal article
File Information	Matsuya Y_2020_Phys.Med.Biol.pdf

Hokkaido University Collection of Scholarly and Academic Papers : HUSCAP

A theoretical cell-killing model to evaluate oxygen enhancement ratios at DNA damage and cell survival endpoints in radiation therapy

Yusuke Matsuya[1,4*], Tatsuhiko Sato[1], Rui Nakamura[2], Shingo Naijo[3], and Hiroyuki Date[4]

[1]Japan Atomic Energy Agency, Nuclear Science and Engineering Center, Research Group for Radiation Transport Analysis, 2-4 Shirakata, Tokai, Ibaraki, 319-1195, Japan
[2]Department of Radiology, Sunagawa City Medical Center, Nishi-4 Kita-3 1-1, Sunagawa, Hokkaiddo, 073-0196, Japan
[3]Graduate School of Health Sciences, Hokkaido University, Kita-12 Nishi-5, Kita-ku, Sapporo, Hokkaiddo, 060-0812, Japan
[4]Faculty of Health Sciences, Hokkaido University, Kita-12 Nishi-5, Kita-ku, Sapporo, Hokkaiddo, 060-0812, Japan
*Corresponding author: matsuya.yusuke@jaea.go.jp (Yusuke Matsuya)

ABSTRACT

Radio-resistance induced under low oxygen pressure plays an important role in malignant progression in fractionated radiotherapy. For the general approach to predict cell killing under hypoxia, cell-killing models (e.g., the Linear-Quadratic model) have to be fitted to *in vitro* experimental survival data for both normoxia and hypoxia to obtain the oxygen enhancement ratio (OER). In such a case, model parameters for every oxygen condition needs to be considered by model-fitting approaches. This is inefficient for fractionated irradiation planning. Here, we present an efficient model for fractionated radiotherapy the integrated microdosimetric-kinetic model including cell-cycle distribution and the OER at DNA double-strand break endpoint (OER_{DSB}). The cell survival curves described by this model can reproduce the *in vitro* experimental survival data for both acute and chronic low oxygen concentrations. The OER_{DSB} used for calculating cell survival agrees well with experimental DSB ratio of normoxia to hypoxia. The important parameters of the model are oxygen pressure and cell-cycle distribution, which enables us to predict cell survival probabilities under chronic hypoxia and chronic anoxia. This work provides biological effective dose (BED) under various oxygen conditions including its uncertainty, which can contribute to creating fractionated regimens for multi-fractionated radiotherapy. If the oxygen concentration in a tumor can be quantified by medical imaging, the present model will make it possible to estimate the cell-killing and BED under hypoxia in more realistic intravital situations.

I. INTRODUCTION

In radiation therapy, hypoxia decreases the radio-sensitivity of cancer cells, and has a critical role in malignant progression.[1,2] The degree of the radio-resistance induced under an oxygen (O_2) concentration of less than 20% is generally evaluated by oxygen enhancement ratio (OER) defined as the ratio between the dose under hypoxic conditions and the dose in the presence of oxygen for the same biological effect.[3,4] The Linear-Quadratic (LQ) model[5-9] is generally applied to the *in vitro* dose-response curve on cell survival to obtain the OER values under various oxygen coditions.[3,10,11]

The OER obtained from cell survival depends largely on the cell survival level (e.g., 10% or 37% cell survival),[12] because the dose-response curve exhibits a linear-quadratic feature in the relation between absorbed dose and logarithm of cell survival.[13] Furthermore, the shape of the cell survival curve changes depending on the period of time that the cells are exposed to hypoxic conditions (acute or chronic).[14,15] This is believed to be induced by a change in cell-cycle phase when irradiated.[3,15] For this reason, the parameters in the LQ model[5-9] have to be obtained by fitting the models to experimental data for various hypoxic conditions including reoxygenation. However, such fitting procedures to various experimental data make the LQ model inefficient for predicting cell survival curve. To solve such inefficiency, it is essential to develop a model that can determine the model parameters from limited experimental data under normoxia and predict survival probabilities under any oxygenation pressures. Our interest is thus to develop a theoretical cell-killing model considering oxygen effects, which is able to predict the cell killing for both acute and chronic lower oxygen concentrations.

After irradiation under pressure of O_2 (p_{O_2}) $\geq$ 20%, initial DNA damage which can lead to cell death with a certain probability, i.e. involving a DNA double-strand break (DSB),[16-20] is induced by both direct and indirect effects. Oxygen effects are intrinsically related to indirect effects.[3,12] Oxygen is a mediator inducing DNA damage,[21] in which the interaction of radiation with liquid water (H_2O) produces several types of free radicals, such as the hydroxyl radical (·OH) which is the most reactive with DNA.[22] There are two primary pathways of the indirect effect associated with oxygen effects to yield more strand breaks: one is through sugar peroxyl radicals[20,23]; the other is base-to-sugar radical transfer from ·OH-mediated base radicals.[17,21,24-26] The increase of DNA damage (radio-sensitivity) from these chemical pathways are completed within milliseconds at an early stage of cell life.[21] Therefore, the paucity of radical reactions with DNA in the early stages[1,21,27] leads to reduced cell killing under hypoxia. In these regards, to consider the progression of oxygen effects, a more biologically detailed model based on DNA damage yield than the conventional LQ model[13] is necessary. When compared to many available models for hypoxia,[10,11,28,29] the integrated microdosimetric-kinetic (IMK) model[30-33] has unique features such as involvement of DNA damage kinetics[34,35] and the cell-cycle phase.[31] The model is suitable for estimating radio-sensitivity under chronic lower oxygen pressure. The development for incorporating mechanistically the oxygen effects into the IMK model enables us to evaluate biological effects (e.g., OER value at the cell survival endpoint) with the uncertainties for various oxygen pressures, and can contribute to a better treatment planning for fractionated radiotherapy.

This work proposes an integrated cell-killing model that can reproduce radio-sensitivity for various oxygen conditions. In the improved IMK model, OER is set in the coefficient that accounts for potentially lethal lesions (PLLs). The model can predict biological effective dose (BED) and associated uncertainties, which is useful in fractionated radiotherapy. The model results show that our theoretical cell-killing model for hypoxia makes it possible to estimate the OER value accurately with its uncertainty.

II. MATERIALS AND METHODS

II.A. *Integrated microdosimetric-kinetic model*

The integrated cell-killing model used in this study, so-called "*integrated microdosimetric- kinetic* (*IMK*) *model*",[30-33] is composed of targeted effects and non-targeted effects. The inclusion of the effects has been tested by comparing the outcomes with *in vitro* experimental survival data. Here, the oxygen effect is incorporated into the model for the targeted effects considering microdosimetry,[36] cell recovery during irradiation,[32,35] and cell-cycle distribution.[31] The expression of cell survival with the target effects is summarized below.

In the model for DNA-targeted effects,[31] the cell nucleus as a target of radiation is divided into a number of micron-order sections called domains,[37] while sub-lethal and lethal lesions so called potentially lethal lesions (PLLs) and lethal lesions (LLs) are assumed for describing DNA damage repair kinetics after irradiation.[37] The domains may be interpreted as interphase chromosome territories,[38] while PLL and LL may be associated with DNA double-strand breaks (DSBs)[38,39] and unstable chromosome aberrations.[38]

Here, we consider continuous irradiation[31,40] with a relatively short time of dose-delivery T (h) at constant dose-rate $\dot{D}$ (Gy/h)[35] in air (p_{O_2}=20%). Assuming that the time courses of PLLs and LLs during irradiation as well as after irradiation are given by: (i) transformation from a PLL to a LL, which may occur at a constant rate a (h^{-1}), (ii) interaction of two PLLs, which may transform into a LL at a constant rate b_d (h^{-1}), (iii) repair of a PLL, which can occur at constant rate c (h^{-1}).[30,31,35] In addition, the cell surviving fraction S as a function of absorbed dose D with the Lea-Catcheside time factor F is deduced as

$$\begin{aligned} -\ln S &= (\alpha_0 + \gamma\beta_0)\dot{D}T + \frac{2\beta_0}{(a+c)^2T^2}\left[(a+c)T + e^{-(a+c)T} - 1\right](\dot{D}T)^2 \\ &= (\alpha_0 + \gamma\beta_0)D + F\beta_0 D^2 \\ &= \alpha D + \beta D^2 \end{aligned} \tag{1}$$

where γ is the microdosimetric quantity ($= y_D/\rho\pi r_d^2$), y_D is the dose-mean lineal energy in keV/μm, r_d and ρ are the radius and density of the domain, respectively (which are set to be r_d = 0.5 μm, ρ = 1.0 g/cm^3),[37,41] $(a+c)$ can be approximated to be c, representing sub-lethal damage repair (SLDR) rate (h^{-1}), $D = \dot{D}T$, $\alpha \equiv \alpha_0 + \gamma\beta_0$,

$$F = \frac{2}{(a+c)^2T^2}\left[(a+c)T + e^{-(a+c)T} - 1\right], \tag{2}$$

and $\beta \equiv F\beta_0$. The Lea-Catcheside time factor F[42] describes the dose-rate effects induced by cell recovery during irradiation.[34] It has been tested and the factor can reproduce experimental cell survival data.[31,32,34,35] Further,

$$\alpha_0 = \frac{a k_d \langle G\rangle}{(a+c)} \cong \frac{a k_d \langle G\rangle}{c} \quad \text{and} \quad \beta_0 = \frac{b_d k_d^2 \langle G^2\rangle}{2p(a+c)} \cong \frac{b_d k_d^2 \langle G^2\rangle}{2p\cdot c}, \tag{3}$$

where k_d is the PLL yield per DNA amount per Gy, <G> is the mean amount of DNA per cell nucleus,

p is the mean number of domains packed in a cell nucleus, $(a+c)$ is the sum of rate constants of a and c. In Eq. (3), $(a+c)$ is approximated by c because the value of a is known to be a few percent of c.[31,37,41] The set of model parameters of (α_0, β_0, $a+c$) is regarded as cell-specific parameters, which can be determined by fitting the model to *in vitro* cell survival data in split-dose and single-dose experiments. It should be noted that the model parameters of (α_0, β_0) depends on cell-cycle phase represented as DNA amount $\langle G \rangle$ and SLDR rate c, as expressed in Eq. (3). The set of model parameters (α_0, β_0) as functions of $\langle G \rangle$ and c can represent the difference of cell survival curves between the plateau phase and the logarithmic growth phase, as reported previously.[31]

II.B. *Incorporation of OER_{DSB} into the IMK model*

Considering strand breaks induced by oxygen-related radicals,[1,21,27] the yield ratio of PLL under any oxygen pressure, p_{O_2} (%), and that by direct and indirect effect under 100% O_2, $\varphi(p_{O_2})$ (in other word, weighting factor of PLL induction by the radicals), is newly introduced in our model. The PLL yield in the previous IMK model can be replaced by $k_d = k_0\varphi(p_{O_2})$, where k_0 is PLL yield per DNA amount per Gy without oxygen-related indirect effects. The OER at the endpoint of DSB (OER_{DSB}) is defined by the ratio,

$$\mathrm{OER}_{\mathrm{DSB}}(p_{O_2}) = \frac{k_0\varphi(100\%)}{k_0\varphi(p_{O_2})}. \quad \because\ \mathrm{OER}_{\mathrm{DSB}}(p_{O_2}) \geq 1.0, \tag{4}$$

where $\varphi(100\%)$ is for oxygen p_{O_2} (= 100%), and $\varphi(p_{O_2})$ is for a lower oxygen concentration compared to $\varphi(100\%)$. Throughout, we consistently refer to the oxygen concentration of $p_{O_2} \geq 20\%$ as oxic condition. By incorporating the $OER_{DSB}(p_{O_2})$ into the expression of PLL yield described in Eq.(3), the cell-specific parameters of (α_0, β_0) and surviving fraction can be re-expressed as follows,

$$\alpha_0^* = \frac{\alpha_0}{\mathrm{OER}_{\mathrm{DSB}}(p_{O_2})} \quad \text{and} \quad \beta_0^* = \frac{\beta_0}{[\mathrm{OER}_{\mathrm{DSB}}(p_{O_2})]^2}, \tag{5}$$

$$-\ln S = \left(\alpha_0^* + \gamma\beta_0^*\right)D + F\beta_0^* D^2. \tag{6}$$

Here, it is noted that the parameters α_{0*} and β_{0*} are cell specific, and OER is the value as a function of p_{O_2} at the endpoint of DSB as denoted by $OER_{DSB}(p_{O_2})$.

For the dependency of p_{O_2} on the OER_{DSB}, we used the traditional Alper and Howard-Flanders model.[43] This model has been developed by Alper and Howard-Flanders[43] to describe the relationship between radiosensitivity and oxygen concentration. The model function is given by

$$\mathrm{OER}_{\mathrm{DSB}}(p_{O_2}) = \frac{p_{O_2} + p_{O_2\mathrm{half}}}{p_{O_2} + p_{O_2\mathrm{half}} \cdot \mathrm{OER}_{\mathrm{DSB}}(0\%)^{-1}} \tag{7}$$

where $OER_{DSB}(0\%)$ is the maximum OER_{DSB} under the condition of p_{O_2} = 0%, and $p_{O_2\mathrm{half}}$ is the oxygen pressure in % corresponding to the half effect on radio-sensitivity. It should be noted that once the set of model parameters (α_0, β_0, $OER_{DSB}(0\%)$, $p_{O_2\mathrm{half}}$) is determined by a fitting approach, the set of cell-specific parameters considering OER_{DSB} (α_{0*}, β_{0*}) and cell survival probability S under any oxygen pressure, p_{O_2}, can be derived using Eqs. (5) and (6).

II.C. *Determination of model parameters by MCMC*

To test the present model expressed by Eqs. (4)-(7), the model was applied to experimental survival of CHO-K1 cells after the exposure to 250 kVp X-rays under various oxygen conditions acutely created (p_{O_2} = 0%, 0.5%, 20%).[14,15] Among the three tested oxygen concentrations, the cell-cycle phase remains almost unchanged,[15] and the cell-cycle dependency can thus be ignored. To obtain the model parameters, we simultaneously fitted the IMK model to experimental data under normoxia and acute low oxygen conditions. The model consists of six parameters of (α_0, β_0, γ, $(a+c)$, $OER_{DSB}(0\%)$, $p_{O_2,half}$) as expressed in Eqs. (5) and (6). Among them, because γ is a physical parameter based on the radiation track structure,[44] its value for 250 kVp X-rays is obtained from a previous report on Monte Carlo simulation for radiation transport.[34] The set of cell-specific parameters (α_0, β_0, $(a+c)$) for CHO-K1 cells in the logarithmic growth phase, which can be used for testing the present model in comparison with experimental data[14,15], has already been presented in our previous report.[31] Using those parameters[31] as the prior information and the experimental data[14,15], we updated the set of cell-specific parameters (α_0, β_0, $(a+c)$) and determined the chemical-related parameters ($OER_{DSB}(0\%)$, $p_{O_2,half}$) via Markov chain Monte Carlo (MCMC) simulation[35] based on the Bayesian theorem.[45]

In the MCMC approach, the likelihood for logarithm of S was assumed to be a normal distribution as previously reported.[35] The prior information for $p_{O_2,half}$ was also set to be a uniform distribution, while that for $OER_{DSB}(0\%)$ associated with the cell survival data under p_{O_2} = 0% is sampled. After the determination of the five parameters (α_0, β_0, $(a+c)$, $OER_{DSB}(0\%)$, $p_{O_2,half}$), we calculated the cell surviving fraction by the present model (Eqs. (5)-(7)) and compared the results with experimental data taken from the literatures.[14,15]

II.D. *Dependency of oxygen concentration on OER at 10 % cell survival level*

For checking the dependency of p_{O_2} on the traditional OER at 10 % survival level (hereafter noted by OER_{SF10}), we also calculated the model-deduced OER_{SF10} (Eqs. (5)-(7)), and compared with the reference data for photon irradiation.[10,43] Using absorbed dose leading to 10% cell survival as a function of $D_{10}(p_{O_2})$, the OER_{SF10} can be defined by

$$OER_{SF10}(p_{O_2}) = \frac{D_{10}(p_{O_2})}{D_{10}(100\%)}, \tag{8}$$

where $D_{10}(100\%)$ is the D_{10} under an oxygen-rich condition with p_{O_2}=100%.

II.E. *Estimation of cell survival considering cell cycle for chronic hypoxia and reoxygenation*

In order to deal with chronic low oxygen conditions and reoxygenation in fractionated radiotherapy,[3] the dependency of radio-sensitivity on cell-cycle phase[3,15] should be taken into account. For this, we modified the part of the IMK model related to the cell-cycle condition.[31] The parameters of (α_0, β_0) depend on the cell-cycle condition of C_p = ($\langle G\rangle$,$\langle G^2\rangle$, c) as expressed in Eqs. (2) and (3), where $\langle G\rangle$ is the mean DNA amount per nucleus and c is the constant rate of SLDR.[31] In our previous

model[31], $\langle G \rangle$ and $\langle G^2 \rangle$ were calculated from the probability density of G (DNA profile) measured by flow cytometer. However, the cell-cycle information is commonly given by the three phases, G_1, S, and G_2/M. Thus, taking approximation that relative DNA amount of S phase to G_1 phase is 1.5, we tried to obtain $\langle G \rangle$ and $\langle G^2 \rangle$. Here, let f_{G1}, f_S and $f_{G2/M}$ be the fractions of G_1, S and G_2/M phases, respectively, then $\langle G \rangle$ and $\langle G^2 \rangle$ can be obtained from the cell-cycle fractions according to the following formulae,

$$\langle G \rangle = G_{G1} f_{G1} + G_S f_S + G_{G2/M} f_{G2/M} \tag{9a}$$

$$\langle G^2 \rangle = G_{G1}^2 f_{G1} + G_S^2 f_S + G_{G2/M}^2 f_{G2/M}, \tag{9b}$$

where G_{G1}, G_S and $G_{G2/M}$ are DNA amount per nucleus for G_1, S and G_2/M phase (= 1.0, 1.5 and 2.0 as the relative G values for simplicity), respectively. Meanwhile, the SLDR rate of c depends on the fraction of cells in S phase,[31] which is written by

$$c = c_0 + \frac{dc}{df_S} f_S. \tag{10}$$

Here, c_0 is the intrinsic SLDR rate independent of f_S, and dc/df_S is the differential rate of SLDR per f_S, previously given as 0.0287 ± 0.0128 in h^{-1}/% for the CHO-K1 cells.[31]

Using the values of $OER_{DSB}(p_{O_2})$ and $C_p = (\langle G \rangle, \langle G^2 \rangle, c)$, we estimated survival curves for various oxygen conditions, i.e., chronic lower oxygen (p_{O_2} = 0%, 0.5%) and reoxygenation (p_{O_2} = 20%).

II.F. *Biological effective dose*

The α/β value is characterized on the basis of the linear-quadratic relation as functions of dose-delivery time [35] and $OER_{DSB}(p_{O_2})$. We calculated the α/β and the BED values by the following equations,

$$\frac{\alpha}{\beta} = \frac{\alpha_0^*}{F\beta_0^*} + \frac{\gamma}{F}, \tag{11}$$

$$\mathrm{BED} = nD_n \left(1 + \frac{D_n}{\alpha/\beta}\right), \tag{12}$$

where D_n is the absorbed dose per fraction and n is the number of fractions in multi-fractionated radiotherapy. It should be noted that this work does not consider repopulation during fractionated irradiation.[46] We calculated the uncertainty of BED as well by utilizing the MCMC method.[35]

III. RESULTS AND DISCUSSION

III.A. *Validation of the proposed model considering OER_{DSB}*

Figure 1 shows the comparison of the present model with experimental data.[14,15] The model parameters (α_0, β_0, γ, $(a+c)$, $OER_{DSB}(0\%)$, $p_{O_2,half}$) determined by MCMC simulations are listed in Table I. Based on this analysis, $OER_{DSB}(20\%)$, $OER_{DSB}(0.5\%)$ and $OER_{DSB}(0\%)$ were estimated to be 1.02 ± 0.14, 1.50 ± 0.21 and 2.39 ± 0.33, respectively. The coefficient of determination (R^2 value) of

the model curves calculated from the mean values of the parameters was found to be 0.966, which indicates that the inclusion of $OER_{DSB}(p_{O_2})$ works well to reproduce the dose-response curves on the cell survival for acute hypoxic (p_{O2} = 0.5%) and anoxic (p_{O2} = 0%).

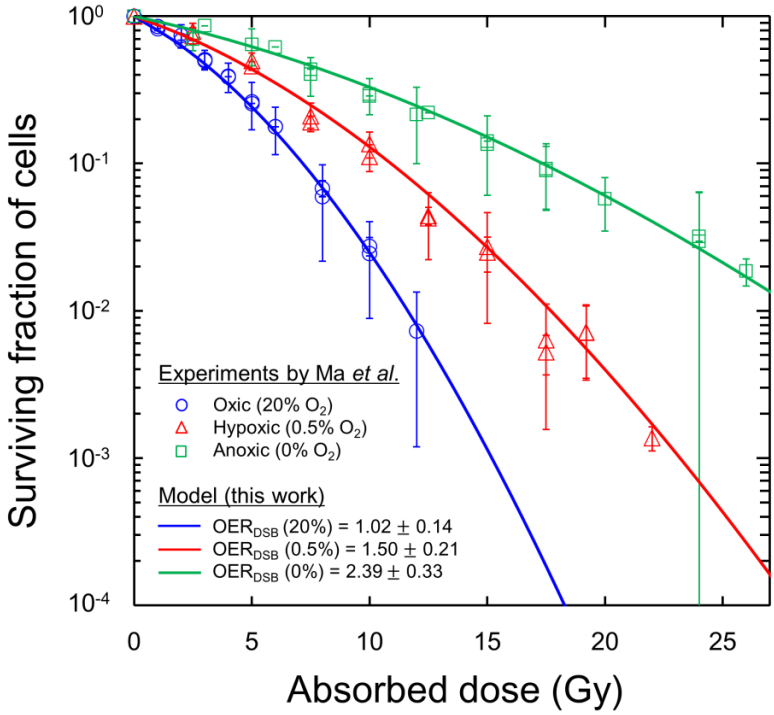

Fig. 1. Cell survival curve for various oxygen concentrations acutely created. The model parameters α_0, β_0, γ, $(a+c)$, OER_{DSB} (0%) and p_{O_2half} which describe the survival curve are listed in Table I. In Fig. 1, the line and symbol represent the calculated curve and the experimental data,[14,15] respectively, for three oxygen pressures, i.e., p_{O_2}= 0%, 0.5% and 20%. Note that the cell-cycle is in a logarithmic growth phase in the cell growth curve.

Table I List of parameters in the IMK model for CHO-K1 cells

Parameter	Values (mean ± sd)	Unit	Meaning	How to determine the value
α_0	$1.81\times10^{-1} \pm 0.15\times10^{-1}$	Gy^{-1}	Coefficient to D (p_{O_2} = 100%)	MCMC with Refs. (14,15)
β_0	$1.89\times10^{-2} \pm 0.17\times10^{-2}$	Gy^{-2}	Coefficient to D^2 (p_{O_2} = 100%)	MCMC with Refs. (14,15)
γ	0.924	Gy	$y_D/\rho\pi r_d^2$ for 250 kVp X-rays	Ref. (34)
$(a+c)$	1.81 ± 0.43	h^{-1}	SLDR rate $[(a+c) \cong c]$	MCMC with Refs. (14,15)
dc/df_S	$2.87\times10^{-2} \pm 1.28\times10^{-2}$	$h^{-1}/\%$	Differential SLDR rate per f_S	Ref. (31)
$OER_{DSB}(0\%)$	2.39 ± 0.33		Maximum OER_{DSB} (p_{O_2} = 0%)	MCMC with Refs. (14,15)
p_{O_2half}	0.67 ± 0.29	%	p_{O_2} leading to half oxygen effects	MCMC with Refs. (14,15)

Published experimental OER_{DSB} values range from 2.0 to 3.2.[47,48] These agree well with the model-deduced OER_{DSB} value of 2.39 ± 0.33, suggesting that the incorporation of the $OER_{DSB}(p_{O_2})$ into the yield of PLLs (k_d) as the enhancement ratio by oxygen-related indirect effects[1,27] is precise,

and the PLL can be linked to lethal lesions caused by DSBs.

To further test this modeling of oxygen effects, we also checked the dependency of oxygen concentration in % on OER at 10% survival level (conventional OER noted by OER_{SF10}). By adapting the Alper and Howard-Flanders model[43] to the present model (Eqs. (5)-(7)), we calculated the dependency of OER_{SF10} on oxygen pressure p_{O_2} as shown in Fig. 2, where solid and dotted lines represent the mean value and 95% CI calculated by the model, respectively. The OER_{SF10} curve calculated by this model agreed well with the OER values in the literatures[10,43] (squares and diamonds in Fig. 2). Focusing on the maximum OER_{SF10} value of p_{O2} = 0%, the $OER_{SF10}(0\%)$ is 2.43 with 26.7% uncertainty (OER_{SF10} = 1.78-3.08: 95% CI), which agrees well with previous *in vitro* OER_{SF10} value of 2.3 ± 0.1[15] and 2.8 ± 0.2[49]) for irradiation with 200 kVp and 250 kVp X-rays in CHO-K1 cells. In addition, even in case of p_{O2} = 100%, the $OER_{SF10}(100\%)$ contains 28.4% uncertainty with 95% CI due to the uncertainties of model parameters [α_0, β_0, $(a+c)$].

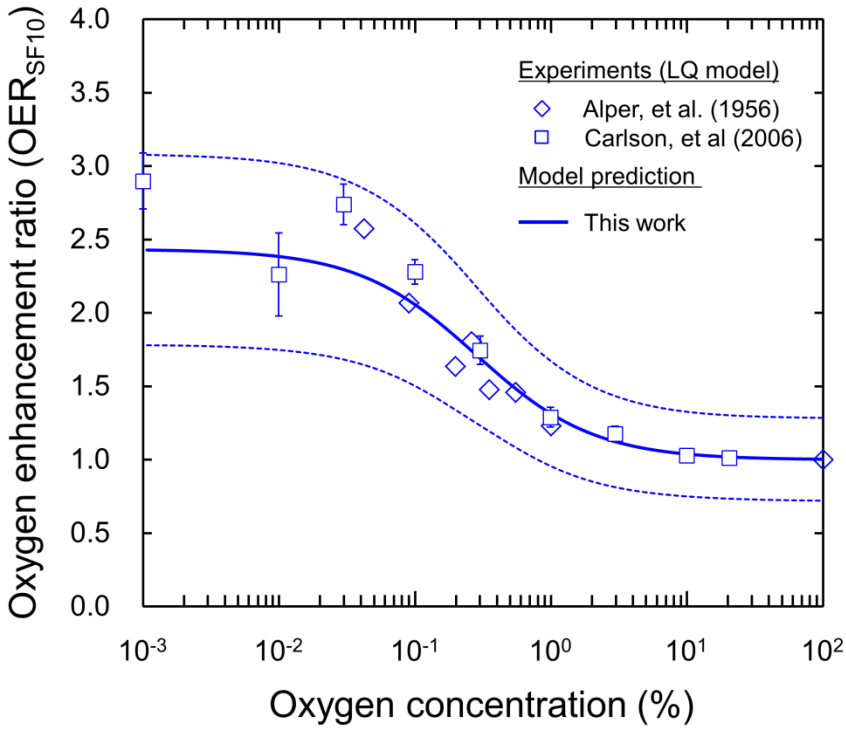

Fig. 2. Dependency of OER_{SF10} on oxygen concentration. Solid and dotted lines represent the mean value and the uncertainty with 95% CI calculated by the present model (Eqs. (5)-(7)), while the symbols (square and diamond) are the reference data on OER at the endpoint of 10% survival level.[10,43] The uncertainty represented by the dotted line was calculated using a MCMC simulation.

In the course of uncertainty evaluation, the OER_{DSB} obtained by applying the present model with oxygen effects to experimental cell survival data[14,15] is consistent with previous data reported in the literatures,[47,49] suggesting that the model accurately describes any radio-sensitivities for a variety of oxygen concentrations, i.e., normoxia, acute hypoxia and acute anoxia.

III.B. *Estimation of cell survival for chronic hypoxia and reoxygenation*

Based on the results as shown in Figs. 1 and 2, the radio-sensitivities (cell survival curves) under chronic hypoxia (p_{O_2}= 0.5%) and anoxia (p_{O_2}= 0%) were calculated. Taking account of experimental cell-cycle data[15] as a potential cause leading to different radio-resistance degrees under acute and chronic anoxia, we calculated the cell survival for two cases of chronic hypoxia (p_{O_2}= 0.5%) and chronic anoxia (p_{O_2}= 0%). Figures 3A and 3B show the cell survival curves under the chronic hypoxia and chronic anoxia, respectively, where the red dotted line is the curve under acute lower oxygen cases, the blue solid line is that under the chronic case, and the black solid line is that under the oxic condition (p_{O_2}= 20%). As shown in Fig. 3A, there is no change of the survival curve between the chronic hypoxia p_{O_2}= 0.5% (black solid line) and the acute hypoxia (red dotted line) because of the similar cell-cycle distribution between acute hypoxia (which has the same distribution as normoxia) and chronic hypoxia (as shown in Table II). Meanwhile, in good agreement with experimental data[15] (circle in Fig. 3B), the radio-sensitivity under chronic anoxia p_{O_2}= 0% (blue solid line in Fig. 3B) is estimated to be higher than acute anoxia due to the reduced fraction of cells in S phase. The model analysis suggests that the change of cell-cycle under chronic anoxia should be considered for reproducing experimental radio-sensitivity under chronic anoxia (p_{O_2}= 0%). If we assume a therapeutic situation, the radio-sensitivity under chronic anoxia (shown in Fig. 3B) should be taken into account for irradiating necrotic anoxic cell population more than 70 μm away from blood capillaries throughout tumour.[3]

Table II Model parameters for various oxygen pressures chronically created

p_{O_2}	Cell-cycle distribution (%)*			Cell condition C_p			Coefficients for dose	
	G_1	S	G_2	relative $\langle G \rangle$ **	relative $\langle G^2 \rangle$ **	c (h^{-1})	α_0*	β_0*
0 %	62.7 ± 1.3	19.6 ± 1.1	17.4 ± 0.8	0.89	0.81	1.13	1.08×10^{-1}	4.28×10^{-3}
0.5 %	36.6 ± 2.3	42.4 ± 1.2	20.4 ± 1.5	0.99	0.98	1.78	1.19×10^{-1}	8.04×10^{-3}
20 %	34.4 ± 3.0	43.1 ± 2.5	21.8 ± 0.7	1.00	1.00	1.80	1.78×10^{-1}	1.89×10^{-2}

* Cell-cycle data[15] provided by Ma *et al.* in a private communication.

** The DNA amounts noted as $\langle G \rangle$ and $\langle G^2 \rangle$ were normalized by the values under p_{O_2} = 20%.

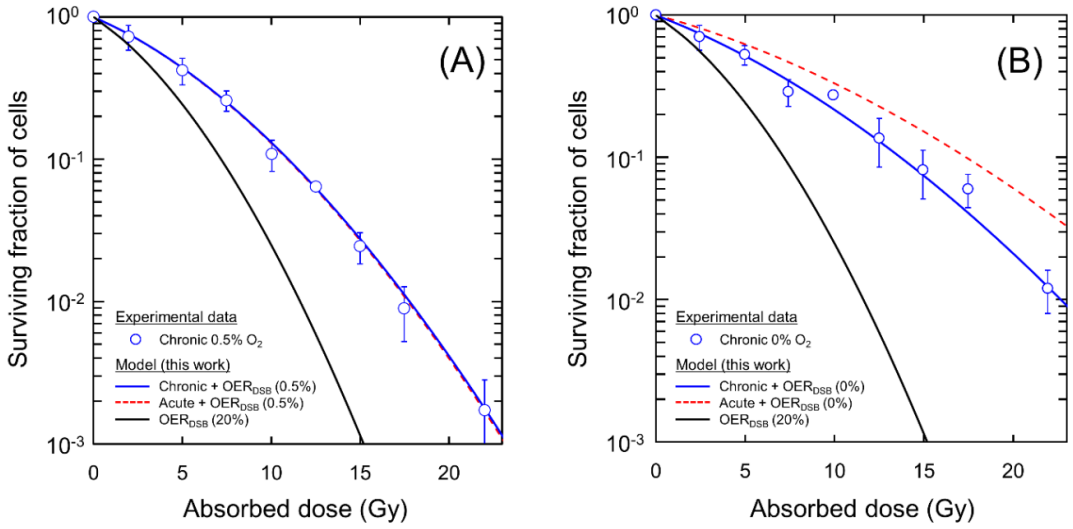

Fig. 3. Estimation of cell survival curve under chronic hypoxia and anoxia: (A) chronic hypoxia (p_{O_2}= 0.5%) and (B) chronic anoxia (p_{O_2}= 0%). The curves in Fig. 3 were predicted by using Eqs. (5)-(7), (9), (10) and Table I and II, where the red dotted line is the curve under acute lower oxygen case, the blue solid line is that under chronic case, and the black solid line is that in air (p_{O_2}= 20%). The R^2 values for chronic hypoxia and anoxia were 0.986 and 0.943, respectively.

We next focused on reoxygenation from chronic cases. According to the experimental cell-cycle dynamics during reoxygenation,[15] the accumulation of cells in G_1 phase under chronic anoxia (p_{O_2}= 0%) decreases with the increase of the cells in S phase, while the cell fraction in S phase increases slightly at 24 h after reoxygenated from the chronic hypoxia (p_{O_2}= 0.5%). Taking these facts into account, we estimated the cell parameters C_p = (<G>, <G^2>, c) as shown in Table III and calculated the cell survival curve for the case of reoxygenation (p_{O_2}= 0% or 0.5% → 20%). Figure 4 shows a comparison between the model calculation and the experimental survival.[15] As expected by the changes of $OER_{DSB}(p_{O_2})$ (i.e., from 2.39 ± 0.33 to 1.02 ± 0.14 for the anoxic case, and from 1.50 ± 0.21 to 1.02 ± 0.14 for the hypoxic case), the calculated radio-sensitivities after reoxygenation are almost the same as that in air (p_{O_2}= 20%), except for the case of 1 h after releasing cultured cells from chronic anoxia to normoxia. Meanwhile, as shown in Fig. 4A, the model exhibits higher radio-sensitivity for case of 24 h after reoxygenation (recovered from chronic hypoxia) than that in air even at the same absorbed dose. Note that this change of radio-sensitivity results from the change in cell-cycle phase from this model estimation.

From these comparisons between the estimation and the experimental data,[15] both oxygen effects, $OER_{DSB}(p_{O_2})$, and cell-cycle phase, C_p, are necessary to predict the difference of radio-sensitivity after reoxygenation from air. However, the model estimation for reoxygenation from chronic anoxia 1 h prior to irradiation (Fig. 4B) shows discrepancies with the experimental data.[15] At this point, incomplete recovery of oxygen concentrations from chronic anoxia is suspected.[50] On the contrary, this model does not consider the time course of oxygen concentrations after returning cells to normoxia. Further investigation and model development for the early phase of reoxygenation from anoxia are necessary for investigating the cause of the discrepancies.

Table III Model parameters for reoxygenation from chronic hypoxia and anoxia

p_{O_2}	t (h)	Cell-cycle distribution (%)*			Cell condition C_p			Coefficients for dose	
		G_1	S	G_2	relative $\langle G \rangle$ **	relative $\langle G^2 \rangle$ **	c (h^{-1})	α_0^*	β_0^*
0%	1 h	60.5 ± 3.5	18.4 ± 4.2	21.1 ± 0.6	0.91	0.85	1.10	2.67×10^{-1}	2.56×10^{-2}
	12 h	42.6 ± 0.9	39.0 ± 3.9	18.3 ± 3.2	0.96	0.93	1.69	1.83×10^{-1}	1.81×10^{-2}
0.5%	0 h	36.6 ± 2.3	42.4 ± 1.2	20.4 ± 1.5	0.99	0.98	1.78	1.77×10^{-1}	1.80×10^{-2}
	24 h	42.3 ± 0.7	36.0 ± 0.3	20.8 ± 1.1	0.97	0.95	1.60	1.93×10^{-1}	1.94×10^{-2}

* Cell-cycle data[15] provided by Ma *et al.* in a private communication.

** The DNA amounts noted as $\langle G \rangle$ and $\langle G^2 \rangle$ were normalized by the values under p_{O_2} = 20%.

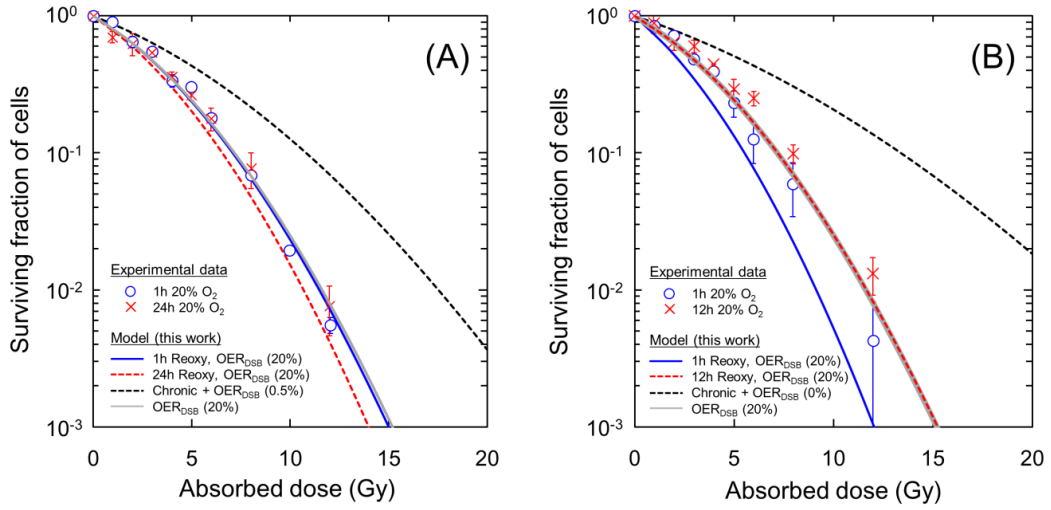

Fig. 4. Estimation of reoxygenation for chronic hypoxia and anoxia: (A) hypoxia (p_{O_2}= 0.5%) and (B) anoxia (p_{O_2}= 0%). As in the same manner as Fig. 3, the curves were estimated based on Eqs. (5)-(7), (9), (10) and Table I, II and III. The R^2 values for 1 h and 12 h after reoxygenation from chronic hypoxia were 0.915 and 0.922, respectively, and those for 1h and 24 h after reoxygenation from chronic anoxia were 0.507 and 0.893, respectively.

III.C. *Uncertainty of BED value for various oxygen pressures*

Assuming realistic clinical cases eliminating cancer in external radiotherapy with 6MV-linac X-rays at a high dose rate of 2.5 Gy/min, we used the set of model parameters [(α_0, β_0, γ, (a+c)) = (0.100 ± 0.027, 0.035 ± 0.002, 0.480, 2.218 ± 0.401)] for non-small lung carcinoma (NSCLC).[35] Using Eqs. (12) and (13), we provide the calculated BED as a function of absorbed dose per fraction (D_n) (total dose 60 Gy[51]) as an example of a clinical case.

Figure 5 shows the dose-dependency of the BED value under three oxygen concentrations, (A) for p_{O_2}= 20, (B) for p_{O_2}= 0.5 and (C) for p_{O_2}= 0%, where the solid line and the dotted line represent the mean value and the 68% uncertainty, respectively. Focusing on the conventional 2 Gy per fraction (Fig. 5(i)), the BED under p_{O_2}= 0% is 76.7 (72.7-84.3: 68% CI) while that under p_{O_2}= 0.5% is 85.1 (79.4-95.6: 68% CI). Based on the outcome of NSCLC in a clinical application,[51] the hypo-fractionated scheme[51,52] i.e., 3 × 20 Gy is a tolerated dose resulting in high local control rates

with minimum normal tissue damage. To this regimen, the BED under p_{O_2}= 0% is 151.7 (130.5-190.8: 68% CI) while that under p_{O_2}= 0.5% is 120.8 (106.3-148.6: 68% CI), as shown in Fig. 5(ii).

As reported previously,[35] the BED value increases as the number of fractions increases in radiotherapy due to dose-rate effects. In addition, it should be noted that the BED as a function of $OER_{DSB}(p_{O_2})$ is newly provided here, showing that the BED is reduced as the oxygen concentration decreases. By taking advantage of the model considering $OER_{DSB}(p_{O_2})$, the mean value and the uncertainty of the biological impacts in fractionated radiotherapy can be calculated for various oxygen concentrations.

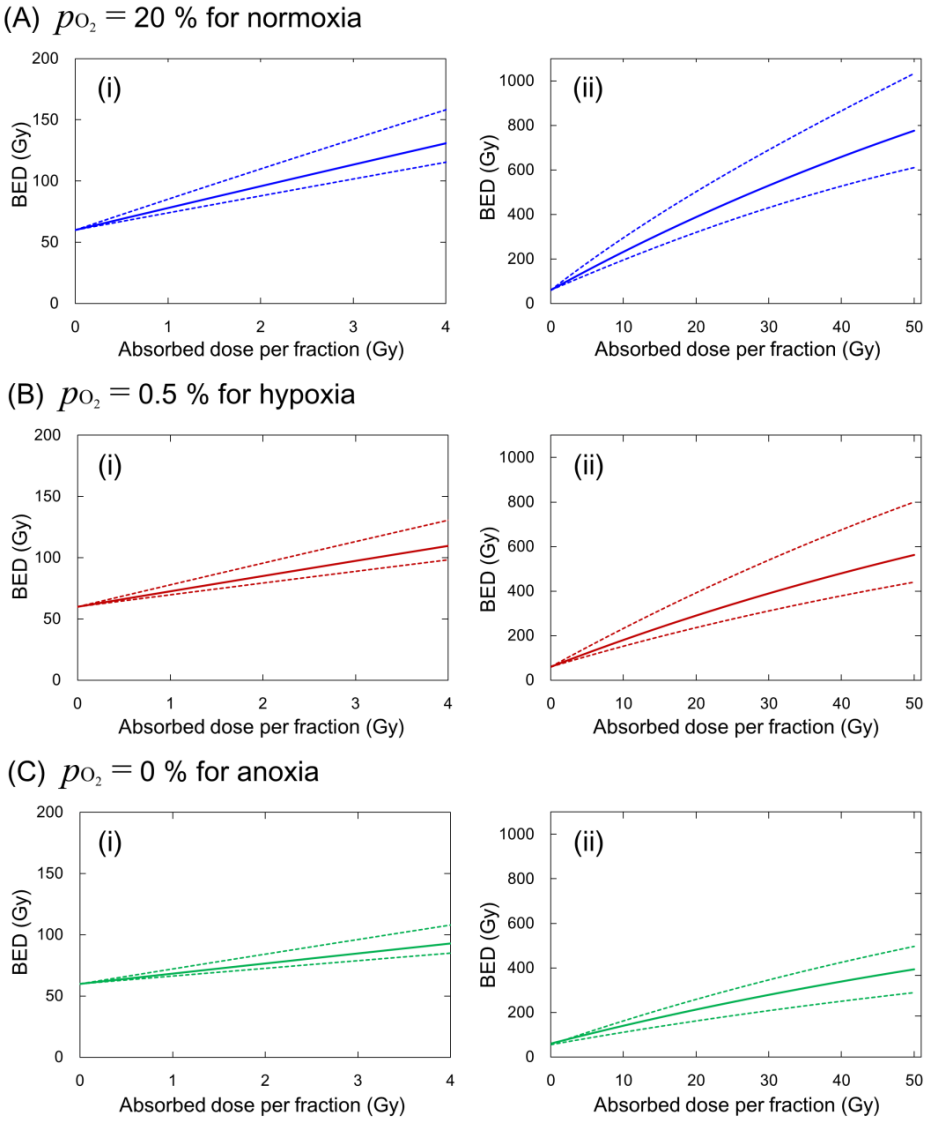

Fig. 5. BED as functions of dose per fraction and oxygen concentration: (A) oxia, (B) hypoxia and (C) anoxia. Left and right panels are the range of low dose per fraction and that of the wide dose range. A realistic clinical case to eliminate NSCLC in the external radiotherapy with 6MV-linac X-rays at 2.5 Gy/min is assumed. Solid line and dotted line represent the mean value and the 68% uncertainty, which are calculated by using the set of model parameters in H1299 cells as reported previously.[35]

The BED value with its uncertainty in tumour cells (shown in Fig. 5) is important information for planning within the fractionated regimen, while the logarithm of cell survival (–log *S*), which can be obtained from Eq. (1), can contribute to pre-clinical evaluation for predicting optical fractionated regimen from the plot of the relation between tumour damage and damage to organ at risk (TO plot).[55-57] The proposed model enables us to predict cell killing and the BED values for various oxygen concentrations (shown in Fig. 1, Fig. 3, Fig.4A and Fig. 5); however, there are still some issues within the model concerning reoxygenation from chronic anoxia (as shown as blue line in Fig. 4B). Assuming the case of the conventional fractionated radiotherapy with 2 Gy per fraction every day (at about 24h intervals), the model can provide the cell survival probability under reoxygenation with high precision (as shown with the red line in Fig. 4B). Further model development for evaluating time course of oxygen concentration is obviously necessary in future study, while the present model development is sufficient for predicting biological effects in fractionated radiotherapy at around 24 h intervals.

IV. CONCLUSION

This work presents a theoretical cell-killing model reproducible for radio-sensitivities for both acute and chronic low oxygen concentrations. By incorporating $OER_{DSB}(p_{O_2})$ into the DNA damage yield term, the present IMK model enables us to calculate the conventional tendency of OER at the endpoint of 10% survival level and cell survival curves flexibly under acute and chronic low oxygen concentrations. The results suggest that oxygen-enhancement to DNA damage and cell-cycle phase are necessary for predicting radio-sensitivity under chronic hypoxia and anoxia. In addition, except for the case of 1 h after releasing cultured cells from chronic anoxia to normoxia, most cases under reoxygenated conditions can also be reproduced by using this model. Focusing on pre-clinical evaluation for fractionated regimens, the biological effectiveness dose (BED) along with its uncertainty can be also calculated by this model considering oxygen effects, which may contribute to making treatment plans in radiation therapy. If the oxygen concentration (p_{O_2}) in the tumor can be quantified by medical imaging, i.e., MRI,[58,59] the cell-killing effects and BED value in various cell lines could be estimated using the OER_{DSB} values presented here. However, the cell-cycle dynamics under chronic anoxia and the time course of oxygen pressure in the cell nucleus after reoxygenated have to be further investigated in future studies.

CONFLICT OF INTEREST

The authors declare that they have no conflict of interest.

ACKNOWLEDGEMENT

The authors sincerely thanks Dr. Tinganelli and Dr. Ma for providing us the raw experimental data to compare with the developed model. We would like to sincerely thank Dr. Kenneth L. Sutherland (Graduate School of Medicine, Hokkaido University, Sapporo, Japan) who kindly spared time for the

English proofreading of the manuscript.

FUNDING

This work was supported by the Japan Society for the Promotion of Science KAKENHI (Grant no. 19K17215).

AUTHOR CONTRIBUTIONS

Y. Matsuya designed this study. Y. Matsuya and T. Sato developed the model. Y. Matsuya, R. Nakamura and S. Naijo performed the MCMC simulation and calculated cell survival. Y. Matsuya wrote the manuscript. H. Date supervised the study. All authors reviewed the manuscript.

REFERENCE

[1] Gray LH, Conger AD, Ebert M, Hornsey S, Scott OC. The concentration of oxygen dissolved in tissues at the time of irradiation as a factor in radiotherapy. *Br. J. Radiol.* 26, 638–648 (1953).

[2] Wright EA, Howard-Flanders P. The influence of oxygen on the radiosensitivity of mammalian tissues. *Acta. Radiol.* 48, 26–32 (1957).

[3] Hall EJ, Giaccia AJ. Oxygen Effect and Reoxygenation. In: Hall EJ, Giaccia AJ. Radiobiology for the Radiologist. 7th ed. Philadelphia: Lippincott Williams & Wilkins, 96-103 (2010).

[4] Horsman, MR, Wouters BG, Joiner MC, Overgaard J. The oxygen effects and fractionated radiotherapy. In: Michael, J., van der Kogel, A.J. (eds). Basic Clinical Radiobiology, 4th edn. London: Hodder Arnold, 207-216 (2009).

[5] Joiner MC. Quantifying cell kill and cell survival. In: Joiner M, van der Kogel AJ (eds). Basic Clinical Radiobiology. London: Edward Arnold, 41–55 (2009).

[6] Bentzen SM, Joiner MC. The linear-quadratic approach in clinical practice. In: Joiner M, van der Kogel AJ (eds). Basic Clinical Radiobiology. London: Edward Arnold, 120–134 (2009).

[7] Marcu L, Eva B, Allen BJ. Biomedical Physics in Radiotherapy for Cancer. Australia: CSIRO Publishing; 2012.

[8] Hall EJ and Giaccia AJ. Time, Dose, and Fractionation in Radiotherapy In: Hall EJ, Giaccia AJ. Radiobiology for the Radiologist 6th ed. Philadelphia: Lippincott Williams & Wilkins, 378–379 (2006).

[9] McMahon, S. J. The linear quadratic model: usage, interpretation and challenges. *Phys. Med. Biol.* 64(1), 01TR01 (2019).

[10] Carlson DJ, Stewart RD, Semenenko VA. Effects of oxygen on intrinsic radiation sensitivity: A test of the relationship between aerobic and hypoxic linear-quadratic（LQ) model parameters. *Med. Phys.* 33(9), 3105-3115 (2006).

[11] Wenz T, Wilkens JJ. Modelling of the oxygen enhancement ratio for ion beam radiation therapy. *Phys. Med. Biol.* 56: 3251-3268 (2011).

[12] Hirayama R. Mechanism of Oxygen Effect for Photon and Heavy-ion Beams. *Jpn. J. Med. Phys.* 34

412 (2): 65–69 (2014).
413 [13]Joiner MC. Quantifying cell kill and cell survival. In: Joiner M, van der Kogel AJ (eds). Basic
414 Clinical Radiobiology. London: Edward Arnold, 41–55 (2009).
415 [14]Tinganelli W, Ma N-Y, Neubeck CV, Maier A, Schicker C, Kraft-Weyrather W, Durante M.
416 Influence of acute hypoxia and radiation quality on cell survival. *J. Radiat. Res.* 54, i23-i30 (2013).
417 [15]Ma N-Y, Tinganelli W, Maier A, Durante M, Kraft-Weyrather W. Influence of chronic hypoxia and
418 radiation quality on cell survival. *J. Radiat. Res.* 54, i13-i22 (2013).
419 [16]Olive PL. The role of DNA single- and double-strand breaks in cell killing by ionizing radiation.
420 *Radiat. Res.* 150 (Suppl.), S42–S51 (1998).
421 [17]Dizdaroglu M, Jaruga P. Mechanisms of free radical-induced damage to DNA. *Free. Radic. Res.* 46,
422 382–419 (2012).
423 [18]Goodhead, DT. Initial events in the cellular effects of ionizing radiations: clustered damage in DNA.
424 *Int. J. Radiat. Biol.* 65(1): 7-17 (1994)
425 [19]Carante MP, Altier S, Bortolussi S, Postuma I, Protti N, Ballarini F. Modeling radiation-induced cell
426 death: role of different levels of DNA damage clustering. *Radiat. Environ. Biophys.* 54: 305–316
427 (2015).
428 [20]von Sonntag C. Free-radical-induced DNA damage and its repair: a chemical perspective. Berlin:
429 Springer (2006).
430 [21]Wardman P. The importance of radiation chemistry to radiation and free radical biology (The 2008
431 Silvanus Thompson Memorial Lecture). *Br. J. Radiol.* 82, 89–104 (2009).
432 [22]Cadet J, Davies KJ, Medeiros MH, Di Mascio P, Wagner JR. Formation and repair of oxidatively
433 generated damage in cellular DNA. *Free. Radic. Biol. Med.* 107,13–34 (2017).
434 [23]Pogozelski WK, Tullius TD. Oxidative strand scission of nucleic acids: routes initiated by hydrogen
435 abstraction from the sugar moiety. *Chem. Rev.* 98, 1089–1107 (1998).
436 [24]von Sonntag C. Carbohydrate radicals: from ethylene glycol to DNA strand breakage. *Int. J. Radiat.*
437 *Biol.* 46, 507–519 (1984).
438 [25]Melvin T, O'Neill P, Jones GD. Influence of nucleic acid base composition on radiation-induced
439 strand breakage in single stranded DNA: a time resolved study. *Int. J. Radiat. Biol.* 66, 499–503
440 (1994).
441 [26]Osman R, Pardo L, Banfelder J, Mazurek AP, Shvartzman L, Strauss R, et al. Molecular
442 mechanisms of radiation induced DNA damage: H-addition to bases, direct ionization and double
443 strand break. *Free. Radic. Res. Commun.* 12–13 Pt 2:465–467 (1991).
444 [27]Jones GD, O'Neill P. Kinetics of radiation-induced strand break formation in single-stranded
445 pyrimidine polynucleotides in the presence and absence of oxygen; a time-resolved light-scattering
446 study. *Int. J. Radiat. Biol.* 59, 1127-1145 (1991).
447 [28]Bopp C, Hirayama R, Inaniwa T, Kitagawa A, Matsufuji N, Noda K. Adaptation of the
448 microdosimetric kinetic model to hypoxia. *Phys. Med. Biol.* 61: 7586–7599 (2016).
449 [29]Alaswad M, Kleefeld C, Foley M. Radiation dose intensity and local tumour control of non-small

cell lung cancer: A radiobiological modelling perspective. *J. Phys. Conf. Ser.* 1248: 012071 (2019).

[30]Matsuya Y, Sasaki K, Yoshii Y, Okuyama G, Date H. Integrated Modelling of Cell Responses after irradiation for DNA-Targeted Effects and Non-Targeted Effects. *Sci. Rep.* 8: 4849 (2018).

[31]Matsuya Y, McMahon SJ, Tsutsumi K, Sasaki K, Okuyama G, Yoshii Y, Mori R, Oikawa J, Prise KM, Date H. Investigation of dose-rate effects and cell-cycle distribution under protracted exposure to ionizing radiation for various dose-rates. *Sci. Rep.* 8: 8287 (2018).

[32]Matsuya Y, McMahon SJ, Ghita M, Yoshii Y, Sato T, Date H, Prise KM. Intensity Modulated Radiation Fields Induce Protective Effects and Reduce Importance of Dose-Rate Effects. *Sci. Rep.* 9: (2019).

[33]Saga R, Matsuya Y, Takahashi R, Hasegawa K, Date H, Hosokawa Y. Analysis of the high-dose range radioresistance of prostate cancer cells, including cancer stem cells based on a stochastic model. *J. Radiat. Res.* 60(3): 298-307 (2019).

[34]Matsuya Y, Tsutsumi K, Sasaki K and Date H. Evaluation of the cell survival curve under radiation exposure based on the kinetics of lesions in relation to dose-delivery time. *J. Radiat. Res.* 56, 90–99 (2015).

[35]Matsuya Y, Kimura T, Date H. Markov chain Monte Carlo analysis for the selection of a cell-killing model under high-dose-rate irradiation. *Med. Phys*. 44(10), 5522-5532 (2017).

[36]ICRU. Microdosimetry. Report 36. International Commission on Radiation Units and Measurements. Bethesda: MD, (1983).

[37]Hawkins RB. A microdosimetric-kinetic model of cell death from exposure to ionizing radiation of any LET with experimental and clinical applications. *Int. J. Radiat. Biol.* 69, 739-755 (1996).

[38]Ballarini F, Altieri S, Bortolussi S, Carante M, Giroletti E, Protti N. The BIANCA model/code of radiation-induced cell death: application to human cells exposed to different radiation types. *Radiat. Environ. Biophys.* 53: 525–533 (2014).

[39]Matsuya Y, Ohtsubo Y, Tsutsumi K, et al. Quantitative estimation of DNA damage by photon irradiation based on the microdosimetric-kinetic model. *J. Radiat. Res.* 55, 484–493 (2014).

[40]Inaniwa, T. Suzuki M, Furukawa T, Kase Y, Kanematsu N, Shirai T, Hawkins RB. Effects of dose-delivery time structure on biological effectiveness for therapeutic carbon-ion beams evaluated with microdosimetric kinetic model. Radiat Res 2013; 180: 44-59.

[41]Hawkins, R. B., Inaniwa, T. A microdosimetric-kinetic model for cell killing by protracted continuous irradiation including dependence on LET I: repair in cultured mammalian cells. *Radiat. Res.* 180, 584-594 (2013).

[42]Brenner, D.J. The linear-quadratic model is an appropriate methodology for determining isoeffective doses at large doses per fraction *Semin. Radiat. Oncol.* 18, 234-239 (2008).

[43]Alper T, Howard-Flanders P. Role of oxygen in modifying the radiosensitivity of *E. coli B*. *Nature* 178, 978–979 (1956).

[44]Nikjoo, H., Uehara, S., Emfietzoglou, D., Pinsky, L. A database of frequency distributions of energy depositions in small-size targets by electrons and ions. *Radiat. Prot. Dosim.* 143(2-4): 145-151

(2011).

[45]Dale AI. Most Honourable Remembrance: The Life and Work of Thomas Bayes. ISBN 0-387-00499-8. Springer, (2003).

[46]Withers HR. The four R's of radiotherapy *Adv. Radiat. Biol.* 5, 241–271 (1975).

[47]Vos O, van der Schans GP, Roos-Verheij WST. Reduction of intracellular Glutathione content and radiosensitivity. *Int. J. Radiat. Biol. Relat. Stud. Phys. Chem. Med.* 50(1), 155-165 (1986).

[48]Kumareswaran R., Ludkovski O., Meng A., Sykes J., Pintilie M., Bristow RG. Chronic hypoxia compromises repair of DNA double-strand breaks to drive genetic instability. *J. Cell Scien.* 125, 189–199 (2011).

[49]Hirayama R, Furusawa Y, Fukawa T, et al. Repair Kinetics of DNA-DSB Induced by X-rays or Carbon Ions under Oxic and Hypoxic Conditions. *J. Radiat. Res.* 46, 325-332 (2005).

[50]Bertuzzia A., Fasano A., Gandolfi A., Sinisgalli C. Reoxygenation and Split-Dose Response to Radiation in a Tumour Model with Krogh-Type Vascular Geometry. *Bulletin Math. Biol.* 70: 992–1012 (2008).

[51]Lagerwaard FJ, Haasbeek CJ, Smit EF, Slotman BJ, Senan S. Outcomes of risk-adapted fractionated stereotactic radiotherapy for stage I non-small-cell lung cancer. *Int. J. Radiat. Oncol. Biol. Phys.* 70, 685–692 (2008).

[52]Marcu L, Eva B, Allen BJ. Biomedical Physics in Radiotherapy for Cancer. Australia: CSIRO Publishing; 2012.

[53]Hattori Y., Yokoya A., Watanabe R. Cellular automaton-based model for radiation-induced bystander effects. *BMC Syst. Biol.* 9:90 (2015).

[54]Jackson RC., Di Veroli GY., Koh S-B., Goldlust I., Richards FM., Jodrell DI. Modelling of the cancer cell cycle as a tool for rational drug development: A systems pharmacology approach to cyclotherapy. *PLoS Comput. Biol.* 13(5): e1005529 (2017).

[55]Sugano Y, Mizuta M, Takao S, Shirato H, Sutherland KL, Date H. Optimization of the fractionated irradiation scheme considering physical doses to tumor and organ at risk based on dose–volume histograms. *Med. Phys.* 42, 6203 (2015).

[56]Mizuta M, Takao S, Date H, Kishimoto N, Sutherland KL, Onimaru R, Shirato H. A Mathematical Study to Select Fractionation Regimen Based on Physical Dose Distribution and the Linear-Quadratic Model. *Int. J. Radiation Oncol. Biol. Phys.* 84.3: 829–833 (2011).

[57]Mizuta M, Date H, Takao S, Kishimoto N, Sutherland KL, Onimaru R, Shirato H. Graphical representation of the effects on tumor and OAR for determining the appropriate fractionation regimen in radiation therapy planning *Med. Phys.* 39, 6791–6795 (2012).

[58]Nöth U, Gröhn P, Jork A, Zimmermann U, Haase A, Lutz J. ^{19}F-MRI in vivo determination of the partial oxygen pressure in perfluorocarbon - loaded alginate capsules implanted into the peritoneal cavity and different tissues. *Mag. Reson. Med.* 42,1039–1047 (1999).

[59]Magat J, Jordan BF, Cron GO, Gallez B. Noninvasive mapping of spontaneous fluctuations in tumor oxygenation using ^{19}F MRI. *Med. Phys.* 37(10), 5434–5441 (2010).